



## LDA MEASUREMENTS OF LOCAL VELOCITIES INSIDE THE GAS PHASE IN HORIZONTAL STRATIFIED/ ATOMIZATION TWO-PHASE FLOW

S. V. PARAS, N. A. VLACHOS and A. J. KARABELAS†

Department of Chemical Engineering and Chemical Process Engineering Research Institute, Aristotle University of Thessaloniki, Univ. Box 455, GR 540 06, Thessaloniki, Greece

(Received 25 July 1996; in revised form 18 September 1997)

**Abstract**—New data on local axial velocities, inside the gas phase in horizontal stratified/atomization air–water pipe flow are reported. Mean local velocities, RMS values and other statistical information have been obtained by analyzing the instantaneous velocity records. From the velocity profiles a secondary flow pattern is inferred with an upward motion at the pipe wall and a downward motion at the vertical pipe centerline. The new measurements are assessed in connection with already reported data of liquid layer characteristics and wall shear stress, obtained under the same flow conditions. The velocity spectra clearly exhibit the influence of the large waves on the gas phase, near the gas–liquid interface; they also suggest that this influence extends up to the top wall of the pipe, probably through the secondary motion inside the gas phase. © 1998 Published by Elsevier Science Ltd. All rights reserved

*Key Words:* air–water flow, stratified/atomization flow, velocity profiles, LDA, secondary flow

### 1. INTRODUCTION

An adequate description of the stratified/atomization flow regime is very useful in understanding atomization processes as well as in modeling the neighbouring (and more complicated) annular flow regime. In particular, knowledge of the flow fields in both the liquid layer and the gas phase is considered a prerequisite to making progress in this direction. Even though several studies have appeared in the literature in recent years, stratified pipe flow with a wavy gas/liquid interface has not been well understood. Andritsos and Hanratty (1987) reviewing available models (mainly concerned with gas/liquid interface stresses) point out their main drawbacks. Two of those are the neglect of possible lateral variation of local shear stress close to the pipe wall, and the assumption of a velocity profile applicable to full pipes. Concerning the liquid layer at the pipe bottom, Paras and Karabelas (1992) reported that only in the immediate vicinity of the solid surface does the liquid motion resemble the well-known behavior of single phase flow, but beyond that the flow field (inside thin liquid films) is strongly influenced by the wavy gas/liquid interface. With regard to the description of the flow field in the gas phase, in horizontal pipes, the literature is very poor even on basic features of the flow, such as the time average velocity distribution, and the possible existence of secondary flow currents. Therefore, the scope of measurements of instantaneous local axial velocities presented here is to gain essential information on flow conditions inside the gas phase that may lead to improved modeling of this complicated flow field.

Velocity measurements of some relevance to this study have been reported by Hanratty and Engen (1957), Cohen and Hanratty (1968), Gayral *et al.* (1979), Fabre *et al.* (1983), Hagiwara *et al.* (1989) and Lee (1992). Their data have been obtained in channels of rectangular cross-section (except those of Hagiwara *et al.* who conducted their experiments in a 49.4 mm i.d. horizontal tube) using techniques such as impact tubes, hot wire and hot film anemometry. These techniques present serious difficulties due to the unavoidable probe interference with the flow and the problems arising from the presence of droplets inside the gas phase. The LDA technique

†To whom correspondence should be addressed.

employed in this work is non-intrusive, permitting measurements very close to the pipe wall (0.1 mm) with very good spatial resolution. Furthermore, the influence of droplets at small concentrations can be effectively eliminated.

Of particular relevance to this research are a few recent studies. The variation of the stream-wise gas velocity was measured with an impact tube, in a horizontal (9.53 cm i.d. pipe) air-water flow, by Dykhno *et al.* (1994). They suggested that, for experiments with little or no entrainment, there exist two or more secondary flow cells with an upward motion at the pipe wall and a downward motion at the center of the pipe. However, in experiments with a relatively large amount of liquid droplets entrained in the gas space a different secondary pattern, with downward motion at the pipe wall and upward motion at the pipe center, was reported to exist and was attributed to the pressure gradients associated with droplet stratification in the gas space. Jayanti *et al.* (1990) studied numerically the secondary flow mechanism, in the gas phase, in a pipe with circumferentially varying wall roughness. They showed that the generated secondary current was too weak to significantly contribute to the film thickness circumferential distribution in horizontal annular flow. Direct measurements of secondary flow in the annular flow regime were made by Flores *et al.* (1995), using a twin axial vorticity meter. The two rotors of the meter remained stationary when only air was passing through the test rig. However, introduction of water into the line caused rotor counter-rotation clearly indicating an upward motion at the pipe wall and a downward one at the pipe center.

In this paper the experimental technique is outlined first and the main results drawn from the local axial velocity measurements are presented and discussed.

## 2. EXPERIMENTAL TECHNIQUE

The velocity measurements were carried out in a horizontal flow loop, described by Paras and Karabelas (1991), where air-water two-phase flow was established in a 50.8 mm i.d. pipe with a 16 m long straight section. The test section was made of high precision glass (Pyrex #7740) with a uniform wall thickness ( $t = 3.81 \text{ mm} \pm 25 \text{ } \mu\text{m}$ ) and a constant refractive index ( $n_{\text{gl}} = 1.474$ ). It was positioned about 300 diameters downstream of the mixing section of the two phases, where the flow is considered to be fully developed.

An LDA set-up, which operates in the fringe mode, was employed in order to make measurements of local axial velocities within the gas phase. A 5 W Argon-Ion laser source was used, having a wavelength of 514.5 nm and a maximum power of 2 W. The green beam from this source is split into two identical beams by an optical arrangement supplied by Dantec. The central beam is fed through a Bragg cell where it is optically shifted by 40 MHz. The two beams are focused, using a 80 mm focal-length lens. The intersecting beams form an ellipsoidal measuring volume (comprised of fringes) with major and minor axes (in air) 91  $\mu\text{m}$  and 23  $\mu\text{m}$ , respectively. The angle of intersection is  $\Theta = 28.1^\circ$  and the optical fringe pattern formed in this measuring volume has a spacing ( $\delta$ ) of 1.06  $\mu\text{m}$  [calibration factor = 1.06 (m/s)/MHz]. Back-scattered light is collected onto a photomultiplier through the same lens. The output signal from the photomultiplier is fed to a Counter Signal Processor (Dantec 55190) which measures the time taken by a particle to cross eight fringes of the measuring volume.

A special support unit for the LDA system was constructed in this laboratory in order to allow precise spatial movement ( $x$ ,  $y$ ,  $\Theta$ ) of the measuring volume. The optical system is fixed onto a vertical adjustable arm and with the use of a balancing weight the system can rotate by  $360^\circ$  around the pipe axis in  $1^\circ$  step intervals. Additionally, two precise  $x$ - $y$  micrometers with 8 cm maximum translation and 10  $\mu\text{m}$  resolution provides the fine horizontal and vertical adjustments. The general arrangement of the LDA system is described in more detail elsewhere (Paras and Karabelas 1992).

Experiments conducted with LDA, especially for the study of gaseous flow, rely on tiny particles (suspended in the continuous medium) which cross the measuring volume to provide velocity information. Therefore, some seeding is always required and it is of critical importance for the quality of measurements. The requirement for good Doppler signals and the dynamics of the flow suggest a particle diameter in the order of the LDA fringe spacing (Drain 1980). Since

Table 1. Main parameters and experimental conditions

Run	$U_G$ (m/s)	$U_L$ (cm/s)	$h_o$ (mm)	Flow regime
KO	6.0	6.0	12.8	wavy stratified
A	11.9	1.9	3.69	wavy stratified
C1	11.9	4.0	4.40	atomization
I	11.9	5.9	6.70	atomization
B1	11.9	8.0	6.50	atomization
A1	11.9	10.0	7.60	atomization
B	16.5	1.9	2.34	atomization
J	16.5	5.9	4.81	atomization

for this experimental set-up the fringe spacing is  $1.06 \mu\text{m}$ , suitable particles must have a diameter of  $0.5$  to  $1 \mu\text{m}$ .

An air jet atomizer (designed and constructed in this laboratory) is used to produce liquid particles of the desired diameter. Small droplets are generated inside a Plexiglas box by passing air through a nozzle, which draws liquid from the reservoir by the venturi effect and breaks it up into a fine spray. In an effort to produce particles suited for such measurements, a special fluid developed by Domnick and Martinuzzi (1994) for seeding purposes is employed. This liquid is a mixture of water and a commercially available "fog-fluid" of unknown exact composition. The main chemical constituent of the fluid is diethylene-glycol and the aerosols thus generated are non-toxic, non-corrosive, non-abrasive and with very suitable light-scattering properties.

There is always the possibility of obtaining erroneous results by measuring, with the LDA technique, gas phase velocity in the stratified/atomization flow regime due to the entrained, in the gas core, droplets that are deposited at the inner tube wall. Laser light passing through such an unevenly wetted wall causes distortion of the measuring volume. To overcome this problem the chemical dichloro-dimethyl-silane is applied on the inner pipe wall to prevent wetting (caused by droplets), without having any effect on the laser beams.

### 3. DESCRIPTION OF EXPERIMENTS

The axial velocity measurements reported here were obtained in an intermediate flow regime in-between "wavy stratified" and "annular" flow. The selected range of superficial liquid

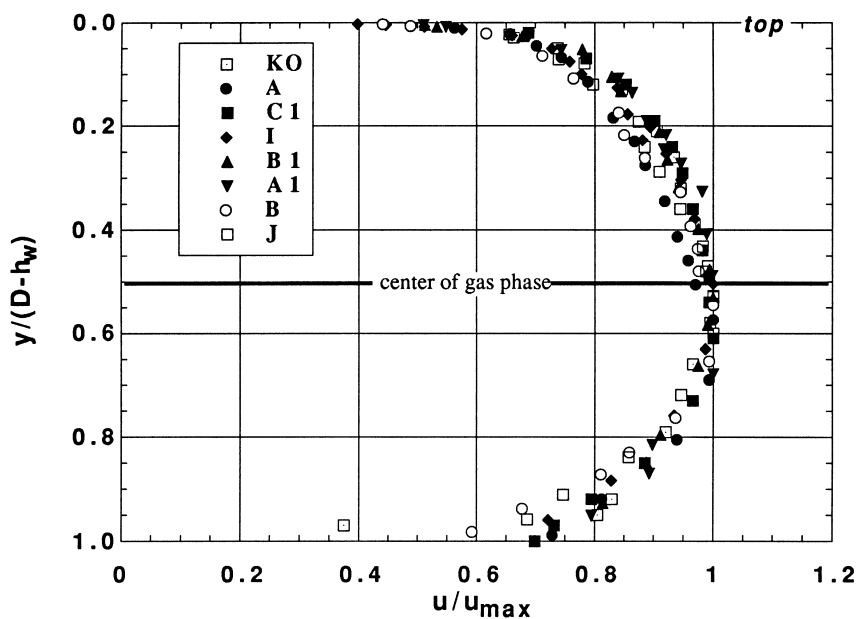


Figure 1. Typical axial velocity profiles along the vertical (all runs). The coordinate  $y$  is measured from the top pipe wall to the top of the waves at the pipe bottom.

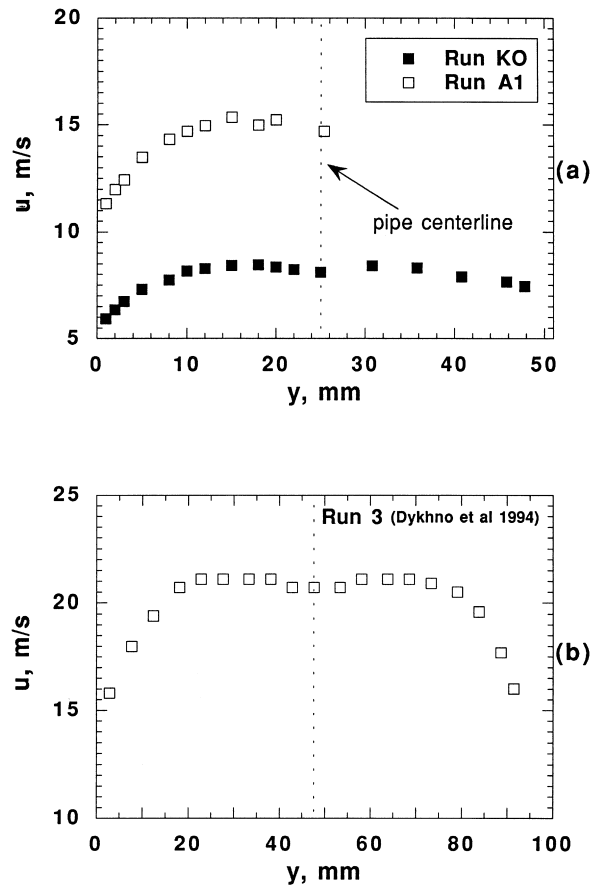


Figure 2. Typical axial velocity profiles, at  $90^\circ$  to the vertical for (a) Run KO and Run A1, (b) Run 3 (Dykhno *et al.* 1994). The coordinate  $y$  corresponds to distance from one side of the pipe inner wall.

velocities ( $U_L$ ) was 2–10 cm/s whereas for the superficial gas velocity ( $U_G$ ) three different cases were tested; namely, 6, 11.9 and 16.5 m/s. The conditions for the various experiments are listed in table 1. Under these conditions, little or no atomization is observed. In general, for a fixed gas flow rate the gas/liquid interface tends to become rougher with increasing liquid flow rate, therefore, larger disturbance waves appear in the interface leading to atomization and droplet entrainment. In addition, the time-averaged film thickness at the pipe bottom,  $h_o$ , is obtained from a companion study by Paras *et al.* (1994) for the same conditions.

For each run, measurements of local instantaneous axial velocity,  $u$ , were made along the vertical pipe diameter, starting at a distance as close as 1 mm from the pipe top and ending 1–2 mm from the air/water interface to avoid light reflections. Laser light coming from reflections at the interface acts as a spurious “reference beam” reaching the photomultiplier. The resulting signals may be interpreted as differential Doppler signals, leading to erroneous data (Drain 1980). Measurements along the horizontal pipe diameter ( $90^\circ$  to the vertical) were also obtained. However, in Runs B and J no velocity data were taken along the horizontal pipe diameter, since for these particular cases the liquid film climbs up to  $90^\circ$ , due to the higher gas flow rate, thus making LDA measurements impossible. Before the main experiments, the velocity profile in single phase air flow was measured to assess the overall accuracy of the non-intrusive optical technique. Good agreement between the measured values and those predicted by the well-known universal velocity profile was obtained.

In these measurements the mean data rate varied from 100–800 Hz, depending on the local mean velocity and the distance from the pipe wall. This sampling frequency was sufficient to allow frequency detection up to 400 Hz. The sample size for each run was 5000 points.

One of the basic problems in LDA is the discontinuity of the signal and the random time intervals between recorded data points, since a data point is collected only when a particle

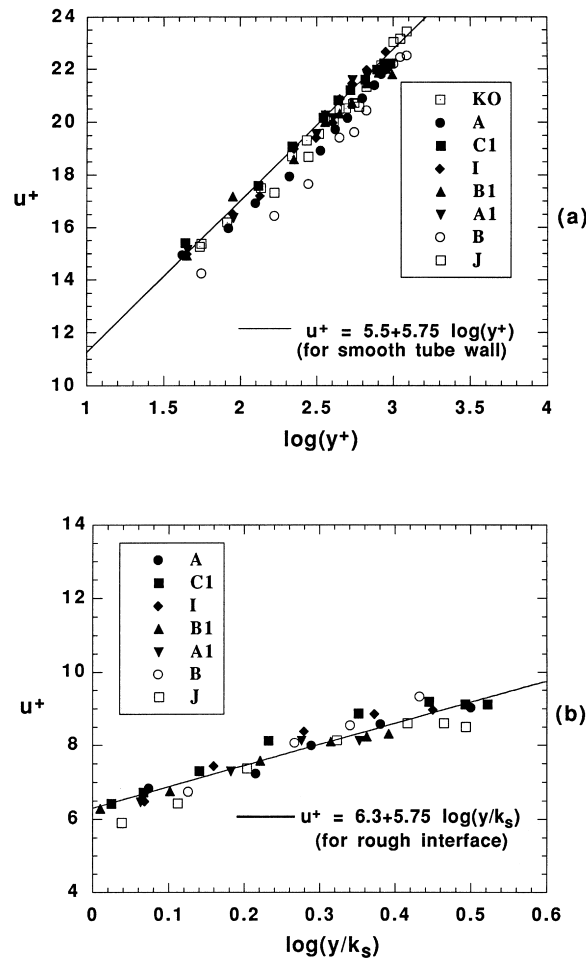


Figure 3. Gas velocity distribution on the vertical pipe diameter (a) near the smooth top pipe wall and (b) near the air-water interface.

passes through the measuring volume. These characteristics can cause “bias” in estimating various statistical quantities, as well as practical problems in computing power spectral densities (PSD) and autocorrelation functions of the fluctuating velocity. Data acquisition and statistical analysis together with the reconstruction of unequally spaced Doppler signals (to overcome the above mentioned problem of the LDA technique) were employed by using an appropriate software package presented elsewhere (Paras and Karabelas 1992).

Furthermore, for the velocity measurements very close to the wavy air-water interface, where the measuring volume was occasionally covered by the waves, a conditional sampling technique was applied to reject erroneous data resulting from the reflections of the laser beams on the interface. In this case the data rate was observed to increase abnormally (order of magnitude excursions) and since the average data rate varied between 100–800 Hz, a threshold level was safely introduced at 1 kHz. Therefore, data acquired with rates above this limit were excluded from the sample. The remaining data were subject to statistical processing and reconstruction.

#### 4. RESULTS

Figure 1 shows typical axial velocity profiles, on the vertical symmetry plane, where one can observe that the maxima of the velocity profiles are displaced slightly *downward* from the center of the gas space. In this figure the vertical coordinate is the distance from the top pipe wall,  $y$ , normalized with the  $(D - h_w)$ , where  $D$  is the pipe diameter and  $h_w$  is the wave height, defined as the vertical distance from the pipe bottom to the top of the waves. Thus  $(D - h_w)$  represents the distance in the gas space between the top of the waves and the pipe top. The velocity,  $u$ , is

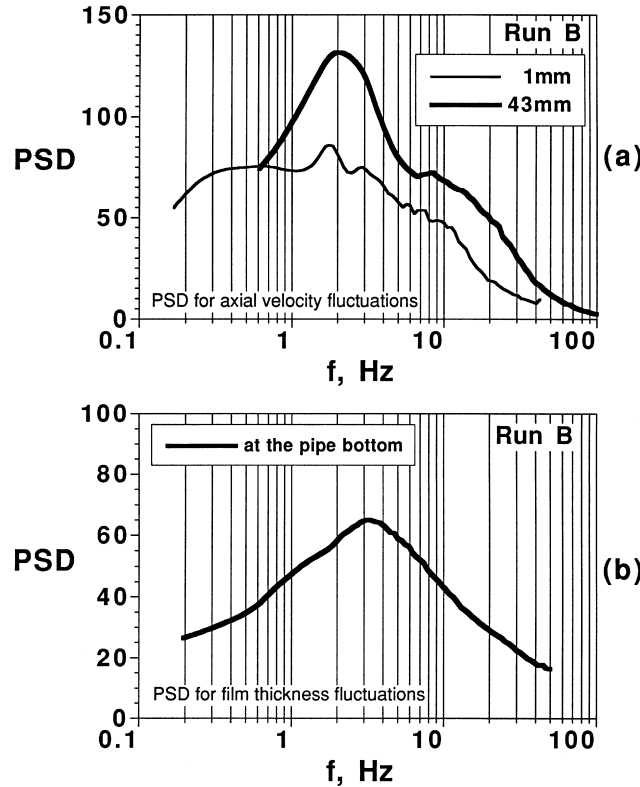


Figure 4. Typical spectra of (a) axial velocity close to the top pipe wall ( $y = 1$  mm) and close to the gas/liquid interface ( $y = 43$  mm), (b) film thickness at the pipe bottom ( $\Theta = 0^\circ$ ). Data from Run B;  $y$  defined as the vertical distance from the top pipe wall.

made dimensionless with its maximum value ( $u_{\max}$ ). Typical axial velocity profiles, at  $90^\circ$  to the vertical, shown in figure 2a, clearly exhibit a “moustache” shape, with a local minimum at the pipe center and two (symmetrically spaced) maxima. A similar shape was obtained by Dykhno *et al.* (1994) for velocity measurements at  $90^\circ$  to the vertical. Figure 2b shows this “moustache” shape of the axial velocity profile for their Run 3, with no or small amount of atomization, as is the case with our experimental data. It should be made clear that in figure 2a and b,  $y$  is measured from one side of the inner pipe wall. The observed type of velocity profiles (both on the vertical symmetry plane and at  $90^\circ$  to the vertical) could be attributed to secondary flow, with downward motion at the vertical symmetry plane and an upward flow at the pipe wall. Such a secondary current is probably generated by the non-uniform liquid film roughness (see Jayanti *et al.* 1990; Dykhno *et al.* 1994; Flores *et al.* 1995), that is the observed decrease in liquid-film wave roughness from the bottom to the top of the pipe (Paras and Karabelas 1991).

For the experiments described in this work, the gas phase is considered to flow through a pipe with an upper surface hydraulically smooth and a lower surface covered by a water film moving slowly relative to the gas phase. Therefore the air–water interface, with respect to gas flow, is considered to be completely rough. Furthermore, near the top pipe wall and near the gas/liquid interface, the axial velocity distribution may be represented by the following dimensionless formulae proposed for single phase flow (Schlichting 1960):

$$u^+ = 5.5 + 5.75 \log(y^+) \quad (\text{smooth wall}) \quad [1]$$

$$u^+ = B + 5.75 \log(y/k_s) \quad (\text{rough interface}) \quad [2]$$

where:  $u^+ = u/u^*$ ,  $y^+ = yu^*/\nu$ ;  $u$  is the local time-averaged axial velocity;  $y$  is the corresponding vertical distance from the top and the bottom pipe wall for the expressions [1] and [2] respectively;  $k_s$  is the apparent interface roughness;  $\nu$  is the air kinematic viscosity; and  $u^*$  is the friction velocity (different for each expression as explained below). The constant  $B$  is generally a

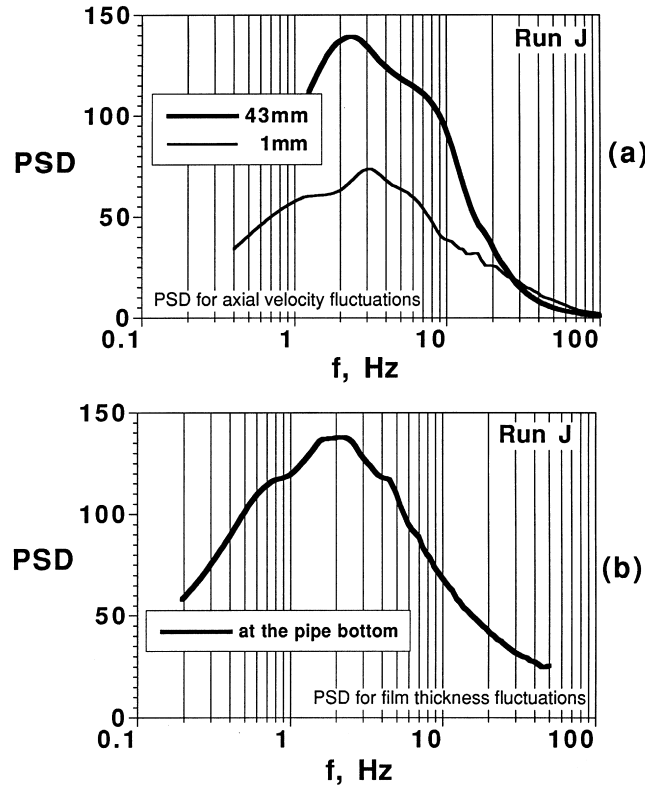


Figure 5. Typical spectra of (a) axial velocity close to the top pipe wall ( $y = 1\text{ mm}$ ) and close to the gas/liquid interface ( $y = 43\text{ mm}$ ), (b) film thickness at the pipe bottom ( $\Theta = 0^\circ$ ). Data from Run J;  $y$  defined as the vertical distance from the top pipe wall.

function of the surface roughness and for our experimental data, in the range of the completely rough regime, it appears to have the value of 6.3, as shown below.

In figure 3 the data points of all runs are presented and correlated quite well (maximum error 10%) with expressions of the form [1] and [2], for both the smooth upper pipe wall and the rough air/water interface, respectively. As regards the former (figure 3a), the data seem to have a tendency to fall below the well-known smooth wall correlation. A small experimental error leading to overprediction of  $u^*$  could have caused the discrepancy. It is difficult, however, with the present set of data, to comment further on this apparent deviation, as it may be within the expected experimental error. The friction velocity ( $u^*$ ) for the smooth wall (expression [1]) is obtained from the single (gas) phase friction factor. Values of friction velocity ( $u^*$ ) for expression [2] (figure 3b) are computed from an average interfacial friction factor ( $f_i$ ), for the rough air/water interface, proposed by Paras *et al.* (1994). Measurements of liquid film thickness, wall shear stress and pressure drop, combined with a better estimation of the gas/liquid interface shape are used for determining  $f_i$ . This is achieved by means of momentum balances for both the liquid and the gas phase. It is pointed out that, in accordance with observations, the time-averaged gas/liquid interface is considered to be "concave" rather than flat (Paras *et al.* 1994) in the above calculations. The values for the apparent interface roughness ( $k_s$ ) are calculated from the evaluated  $f_i$  (using the well known resistance formula for the completely rough regime, Schlichting 1960) and are related to wave characteristics such as roll wave height and intermittency (Paras *et al.* 1994, equation [9]), for the same runs reported here. It will be noted here that data corresponding to Run KO are not included in figure 3b because for this particular experiment it was not possible to determine neither the interfacial friction factor nor the apparent interface roughness, since no measurements of liquid layer characteristics were carried out.

The same well-known logarithmic relations were employed by many other investigators (see Hanratty and Engen 1957; Ellis and Gay 1959; Gayral *et al.* 1979; Sinai 1983; Jayanti *et al.*

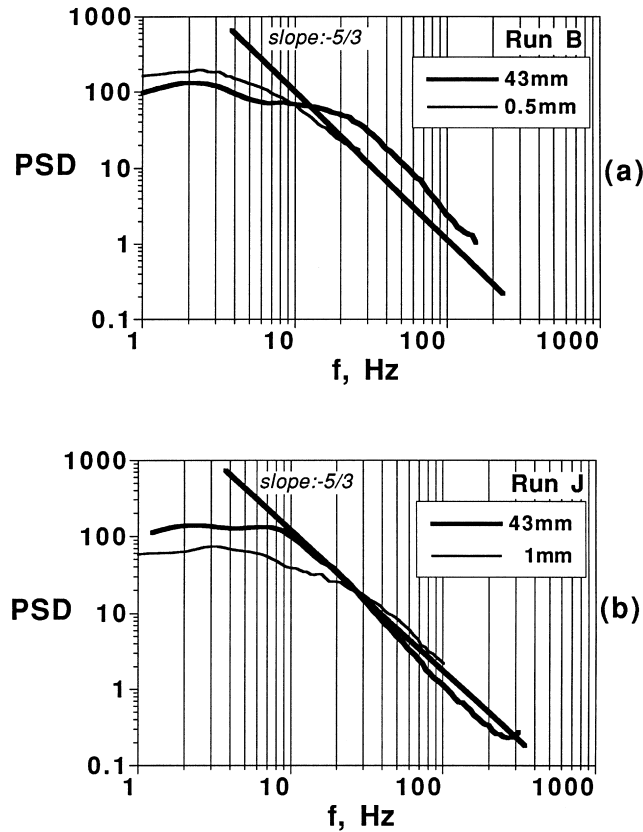


Figure 6. Typical spectra of (a) axial velocity close to the top pipe wall ( $y = 0.5\text{ mm}$ ) and close to the gas/liquid interface ( $y = 43\text{ mm}$ ) in log-log coordinates (Run B), (b) axial velocity close to the top pipe wall ( $y = 1\text{ mm}$ ) and close to the gas/liquid interface ( $y = 43\text{ mm}$ ) in log-log coordinates (Run J). The coordinate  $y$  is defined as the vertical distance from the top pipe wall.

1990) in order to describe the flow field in the gas phase. Hansen and Vested (1991) assumed that the velocity profile in both the gas and the liquid phase could be described by the sum of two logarithmic profiles with the interface treated as a moving wall. This approach provided very good results for smooth stratified flow, whereas for wavy conditions it failed in comparison to the measured values especially near the interface.

Paras *et al.* (1994) reported that liquid thickness and wall shear stress spectra display similarities, clearly showing the influence of interfacial waves on stress at the wall. A similar conclusion is drawn in this work; that is from the calculated spectra (figures 4 and 5) it is clear that there is a significant influence of the large waves on the gas flow, especially near the air/water interface. Most probably the characteristic (modal) values of the velocity spectra near the gas/liquid interface correspond to the frequencies of the large waves in the stratified/atomization flow regime obtained earlier (Paras *et al.* 1994) from film thickness spectra (figures 4b and 5b), for the same runs made here. In support of this suggestion it is noted that the secondary flow is expected to fluctuate apparently due to the variable interfacial roughness (Flores *et al.* 1995). Since this roughness varies with a characteristic frequency corresponding to that of the large waves (Paras *et al.* 1994), the secondary flow fluctuations may be related to that frequency. The form of the spectra of the axial velocity close to the top pipe wall ( $y = 1\text{ mm}$ ), which resembles those obtained near the gas/liquid interface (having the same shape and characteristic frequencies) seems to support this suggestion (figures 4a and 5a). However, this influence of the waves is not observed in the corresponding spectra near the wall for axial velocity measurements inside the liquid layer (Paras and Karabelas 1992).

In logarithmic coordinates, the slope of the PSD curves in the high frequency range is roughly  $-5/3$  close to the top pipe wall and near the interface, as in the case of turbulent single phase flow (figure 6). This result suggests that the main (axial) flow retains the basic features of



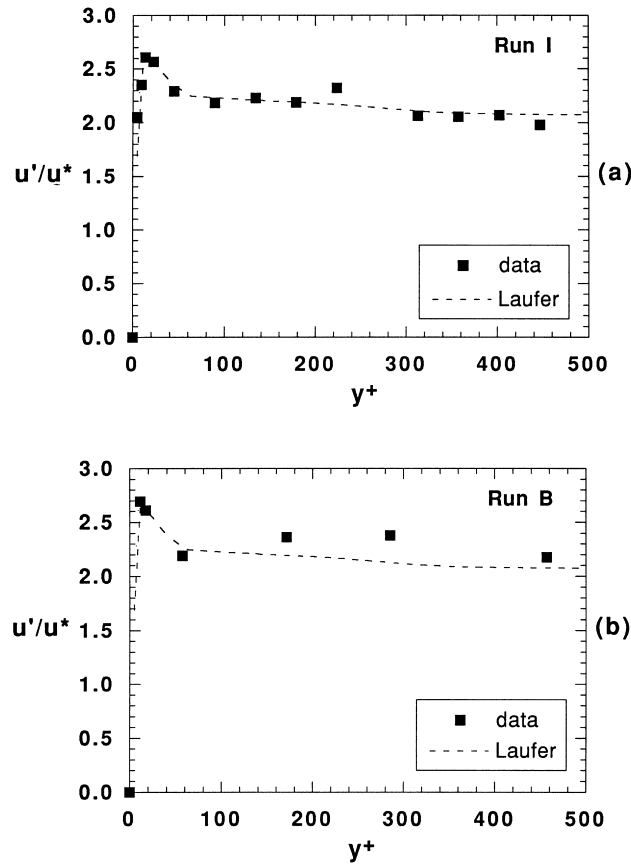


Figure 7. Distribution of turbulence intensity for (a) Run I and (b) Run B. Dashed line corresponds to data by Laufer (1954), for single-phase pipe flow. The  $y$  coordinate is measured from the top pipe wall.

turbulent flow near the top pipe wall as well as close to the air/water interface. It should be pointed out that in this figure data above 100 Hz are not considered reliable, if one takes into account the mean rate of data acquisition in the respective runs.

It is interesting that the distributions of turbulent intensities  $u'/u^*$ , for both runs plotted in figure 7, are in agreement with the well-known data of Laufer (1954) for single phase pipe flow. The maximum value of approximately 2.7 is observed in both cases at distances from the top pipe wall  $y^+ \sim 10-20$ , in accord with the Laufer data. In this figure,  $y^+ = 500$  means that (in the real pipe scale) the local velocity measurement was taken at a distance of  $y = 11$  mm from the top pipe wall. These results again suggest that (at the pipe top) the basic features of turbulent single phase flow are preserved. Figure 8 presents the RMS values ( $u'$ ) of the axial velocity with respect to the distance  $y$  from the top pipe wall, on the vertical symmetry plane. It is clear that the velocity fluctuations are high near the top pipe wall as in measurements in single phase flow (Laufer 1954; Ueda and Hinze 1975). Also the high level of the RMS values, in the space above the gas/liquid interface, is clearly associated with the presence of large waves at the interface and with the air/water interfacial shearing, as one might have expected. In this figure, the minimum RMS values correspond roughly to the maximum time-averaged velocities, obtained slightly below the center of the gas space.

## 5. CONCLUDING REMARKS

The new LDA data in the gas phase of stratified/atomization flow are assessed in connection with already reported data of wavy liquid layer characteristics obtained in the same experimental set-up, under the same conditions, and are found to be consistent. The present experiments were carried out under conditions where a small amount of atomized droplets, or none at all,

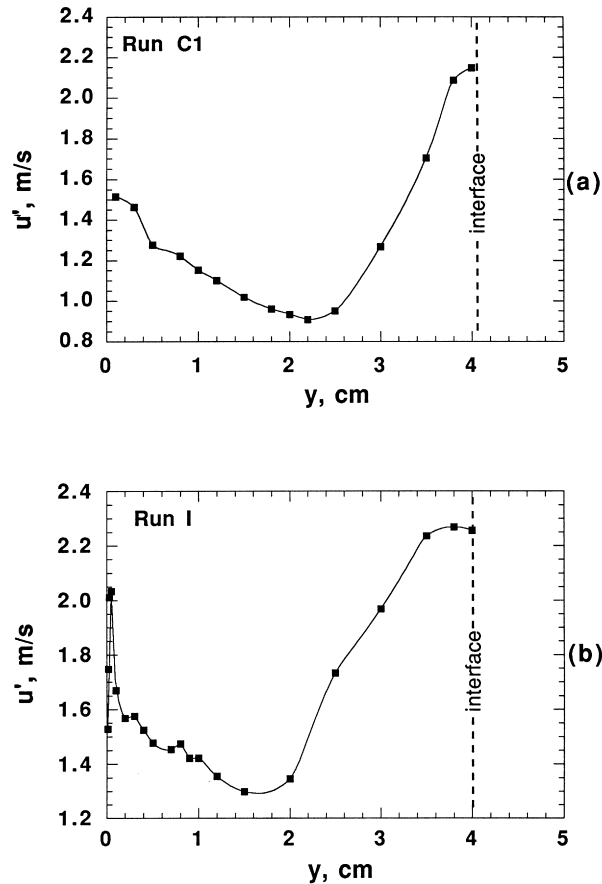


Figure 8. RMS values of the axial velocity ( $u'$ ) on the vertical symmetry plane with  $y$  distance measured from the top pipe wall for (a) Run C1 and (b) Run I.

were entrained in the gas. Under these conditions, the time average velocity profiles on the vertical symmetry plane display a maximum generally below the middle (or center) of the gas space coordinate  $y/(D-h_w)$ . On the contrary, the axial velocity profiles on the horizontal symmetry plane (namely  $90^\circ$  to the vertical) clearly exhibit a “moustache” shape, with a local minimum at the pipe center, and *two* (symmetrically spaced) maxima. These trends are in agreement with those observed in the data by Dykhno *et al.* (1994), strongly suggesting the presence of secondary flow currents. Regarding the structure of such secondary currents, the new data seem to be in agreement with the observations made by Flores *et al.* (1995), that is of two large counter-rotating vortices with respect to the vertical symmetry plane. However, in experiments with extensive atomization, the measured velocity profiles, obtained by Dykhno *et al.*, display a significantly different behavior having their maxima above the center of the gas space.

Well-known forms of the turbulent velocity profile seem to be quite satisfactory for correlating the data, not only at the pipe top but also in the lower strata of gas phase if the equivalent roughness of the wavy interface is properly taken into account. The basic features of single phase pipe flow seem to be preserved at the pipe top, as shown in typical PSD curves and distributions of  $u'$  intensities in the  $y$  direction.

The influence of large waves is quite significant near the gas/liquid interface, as expected. An interesting finding of this study (obtained from the velocity spectra) is that the influence of large waves may extend up to the pipe top (even at  $y \approx 1$  mm), probably through the secondary motion in the gas core.

*Acknowledgements*—Financial support by the European Commission under contracts JOUG-0005-C and JOU2-CT92-0108 are gratefully acknowledged.

## REFERENCES

- Andritsos, N. and Hanratty, T. J. (1987) Influence of interfacial waves in stratified gas-liquid flows. *AIChE J.* **33**, 444–454.
- Cohen, L. S. and Hanratty, T. J. (1968) Effect of waves at a gas-liquid interface on a turbulent air flow. *J. Fluid Mech.* **31**, 467–479.
- Domnick, J. and Martinuzzi, R. (1994) A cheap and effective alternative for particle seeding fluid in LDA-applications. *Experiments in Fluids* **16**, 292–295.
- Drain, L. E. (1980) *The Laser Doppler Technique*. J. Wiley & Sons Ltd, New York.
- Dykhno, L. A., Williams, L. R. and Hanratty, T. J. (1994) Maps of mean gas velocity for stratified flows with and without atomization. *Int. J. Multiphase Flow* **20**, 691–702.
- Ellis, S. R. M. and Gay, B. (1959) The parallel flow of two fluid streams: Interfacial shear and fluid-fluid interaction. *Trans. Instn Chem. Eng.* **37**, 206–213.
- Fabre, J., Masbernat, L. and Suzanne, C. (1983) New results on the structure of stratified gas-liquid flow. *Proc. of 3rd Multiphase Flow & Heat Transfer Conference* **1**, 135–154, Miami Beach, Florida.
- Flores, A. G., Crowe, K. E. and Griffith, P. (1995) Gas-phase secondary flow in horizontal, stratified and annular two-phase flow. *Int. J. Multiphase Flow* **21**, 207–221.
- Gayral, L., Masbernat, L. and Suzanne, C. (1979) Mean velocities and Reynolds stresses in co-current gas-liquid stratified channel flow. Two-phase Momentum, Heat and Mass transfer in Chemical, Process and Energy Engineering Systems. *Durst, Tsiklauri and Afgan* **2**, 921–931.
- Hagiwara, Y., Esmailzadeh, E., Tsutsui, H. and Suzuki, K. (1989) Simultaneous measurement of liquid film thickness, wall shear stress and gas flow turbulence of horizontal wavy two-phase flow. *Int. J. Multiphase Flow* **15**, 421–431.
- Hanratty, T. J. and Engen, J. M. (1957) Interaction between a turbulent air stream and a moving water surface. *AIChE J.* **3**, 299–304.
- Hansen, E. A. and Vested, H. J. (1991) Liquid hold-up, pressure drop, and velocity profiles in steady uniform stratified flow. *J. Energy Resources Technol.* **113**, 87–93.
- Jayanti, S., Wilkes, N. S., Clarke, D. S. and Hewitt, G. F. (1990) The prediction of turbulent flows over roughened surfaces and its application to interpretation of mechanisms of horizontal annular flow. *Proc. R. Soc. Lond. A* **431**, 71–88.
- Laufer, J. (1954) The structure of turbulence in fully developed pipe flow. *Natl. Adv. Comm. Aeronaut.* Tech. Report 1174, 17.
- Lee, S. C. (1992) Interfacial friction factors in countercurrent stratified two-phase flow. *Chem. Eng. Comm.* **118**, 3–16.
- Paras, S. V. and Karabelas, A. J. (1991) Properties of the liquid layer in horizontal annular flow. *Int. J. Multiphase Flow* **17**, 439–454.
- Paras, S. V. and Karabelas, A. J. (1992) Measurements of local velocities inside thin liquid films in horizontal two-phase flow. *Experiments in Fluids* **13**, 190–198.
- Paras, S. V., Vlachos, N. A. and Karabelas, A. J. (1994) Liquid layer characteristics in stratified-atomization flow. *Int. J. Multiphase Flow* **20**, 939–956.
- Schlichting, H. (1960) *Boundary Layer Theory*, 4th edn. McGraw-Hill, New York.
- Sinai, Y. L. (1983) A Charnock-based estimate of interfacial resistance and roughness for internal, fully-developed, stratified, two-phase horizontal flow. *Int. J. Multiphase Flow* **9**, 13–19.
- Ueda, H. and Hinze, J. O. (1975) Fine-structure in the wall region of a turbulent boundary layer. *J. Fluid Mech.* **67**, 125–143.